



Published in final edited form as:

Proc SPIE Int Soc Opt Eng. 2020 February ; 11315: . doi:10.1117/12.2566505.

Integrative radiomic analysis for pre-surgical prognostic stratification of glioblastoma patients: from advanced to basic MRI protocols

Spyridon Bakas^{1,†}, Gaurav Shukla, M.D.^{1,†}, Hamed Akbari, M.D.^{1,†}, Guray Erus¹, Aristeidis Sotiras², Saima Rathore¹, Chiharu Sako¹, Sung Min Ha², Martin Rozycki³, Ashish Singh¹, Russell Shinohara⁴, Michel Bilello, M.D.¹, Christos Davatzikos¹

¹University of Pennsylvania, Department of Radiology, Center for Biomedical Image Computing and Analytics, University of Pennsylvania, USA

²Washington University, Department of Radiology, St. Louis, MO, USA

³CVS Health, Boston, MA, USA

⁴University of Pennsylvania, Department of Biostatistics, University of Pennsylvania, USA

Abstract

Glioblastoma, the most common and aggressive adult brain tumor, is considered non-curative at diagnosis. Current literature shows promise on imaging-based overall survival prediction for patients with glioblastoma while integrating advanced (structural, perfusion, and diffusion) multipara metric magnetic resonance imaging (Adv-mpMRI). However, most patients prior to initiation of therapy typically undergo only basic structural mpMRI (Bas-mpMRI, i.e., T1, T1-Gd, T2, T2-FLAIR) pre-operatively, rather than Adv-mpMRI. Here we assess a retrospective cohort of 101 glioblastoma patients with available Adv-mpMRI from a previous study, which has shown that an initial feature panel (IFP) extracted from Adv-mpMRI can yield accurate overall survival stratification. We further focus on demonstrating that equally accurate prediction models can be constructed using augmented feature panels (AFP) extracted solely from Bas-mpMRI, obviating the need for using Adv-mpMRI. The classification accuracy of the model utilizing Adv-mpMRI protocols and the IFP was 72.77%, and improved to 74.26% when utilizing the AFP on Bas-mpMRI. Furthermore, Kaplan-Meier analysis demonstrated superior classification of subjects into short-, intermediate-, and long-survivor classes when using AFP on Basic-mpMRI. This quantitative evaluation indicates that accurate survival prediction in glioblastoma patients is feasible by using solely Bas-mpMRI and integrative radiomic analysis can compensate for the lack of Adv-mpMRI. Our finding holds promise for predicting overall survival based on commonly-acquired Bas-mpMRI, and hence for potential generalization across multiple institutions that may not have access to Adv-mpMRI, facilitating better patient selection.

* sbakas@upenn.edu.

† These authors contributed equally to this work.

Keywords

radiomics; glioblastoma; survival; prediction; prognosis; multivariate

1. INTRODUCTION

Glioblastoma is the most aggressive malignant primary adult tumor of the central nervous system, with a median survival of 14–16 months if standard of care treatment is followed, and 4 months otherwise (1). Glioblastomas exhibit highly heterogeneous histological and molecular profiles, reflected in their radio phenotypes (2), which includes various sub-regions, i.e. enhancing (ET), non-enhancing (NET) tumor, as well as the peritumoral edematous/invaded tissue (ED) (3).

There is increasing evidence that quantitative analysis of radiographic (i.e., radiomic) features extracted from multi-parametric magnetic resonance imaging (mpMRI) scans can reveal sub-visual cues, which can be associated with prediction of clinical outcomes and molecular characteristics (2, 4–8). However, most studies that investigated the predictive value of imaging compared with clinical and molecular parameters used imaging data obtained from advanced acquisition protocols (Adv-mpMRI, i.e., T1, T1-Gd, T2, T2-FLAIR, DSC, DTI), which are not yet widely incorporated into clinical practice (9). Therefore, many of the promising findings may not be easily generalizable across institutions.

To address this limitation, this study focused on evaluating the feasibility and performance of predicting the overall survival (OS) of glioblastoma patients using exclusively pre-operative baseline basic structural mpMRI scans (Bas-mpMRI, i.e., T1, T1-Gd, T2, T2-FLAIR), via quantitative radiomic analysis. Towards this aim, extensive sets of radiomic features from various glioblastoma sub-regions (ED, ET, NET), describing mpMRI signals, were integratively analyzed using multivariate pattern analysis and machine learning methods. Specifically, we evaluate a retrospective cohort of glioblastoma patients from a previous study that has shown accurate prognostic stratification utilizing Adv-mpMRI, and we focus on demonstrating that equally accurate prediction models can be constructed utilizing exclusively Bas-mpMRI.

2. METHODS

2.1 Dataset

We used a retrospective cohort of 101 patients diagnosed with primary (*de novo*) glioblastoma at the Hospital of the University of Pennsylvania (HUP) between 2006 and 2013 (6). These patients were scanned pre-operatively using an Adv-mpMRI protocol of 6 modalities, comprising native (T1) and contrast-enhanced (T1-Gd) T1-weighted, T2-weighted (T2), T2 Fluid-Attenuated Inversion Recovery (T2-FLAIR), Diffusion Tensor Imaging (DTI), and Dynamic Susceptibility Contrast (DSC) MRI volumes. Mean and median patient age was 62.5 and 61.4 years, respectively (range: 22–88.6 years). No randomization method was used for allocating samples to experimental groups.

The details of this cohort have been described previously (6). The protocol was approved by the Institutional Review Board at HUP, and informed consent was obtained from all subjects. Patients were divided in short-survivors (<12mts) and long-survivors (>14mts). These thresholds were based on equal quantiles from the median OS (~13mts) to avoid potential bias towards one of the survival groups. The median OS of the described cohorts is not significantly different from the median survival of glioblastoma patients reported in the literature (10, 11).

OS was defined as the duration of time between the establishment of diagnosis and the date of death. Kaplan-Meier (KM) curves were generated for the depiction of OS based on the result of each predictive model, as well as for the true classification. The Cox proportional hazards model was used to estimate the hazard ratio of death between groups (12).

2.2 Segmentation of Tumor Sub-regions

All mpMRI volumes were preprocessed as mentioned in (13), and all histograms of all patients were matched to the corresponding modality of a reference patient. The Bas-mpMRI scans were used to segment the various tumor sub-regions, using a hybrid generative-discriminative method named GLISTRboost (14). The generative part incorporates a glioma growth model (15), and it is based on an Expectation-Maximization framework to segment brain volumes into tumor (i.e., ET, NET and ED) and healthy tissue labels (e.g., white and gray matter). The discriminative part is based on a gradient boosting (16) multiclass classification scheme, trained on the Brain Tumor Segmentation (BraTS) challenge (3) data, to refine tumor labels based on population data. Lastly, a Bayesian strategy (17) is employed to finalize the segmentation labels based on patient-specific statistics. The derived segmentation labels were considered final after their evaluation and manual revision, when needed, by an expert board-certified neuroradiologist (M.B.).

2.3 Radiomic Features

The Cancer Imaging Phenomics Toolkit (CaPTk) (18) was used to extract 1612 features, for all available mpMRI, based on the tumor sub-regions, while following the Imaging Biomarker Standardization Initiative (IBSI) definitions (19). These features comprised i) intensity, ii) volume, iii) histograms (6), iv) spatial information (20), v) glioma growth model parameters (21), as well as vi) morphology (22) and vii) texture (19) parameters, including features based on Grey-Level Co-occurrence Matrix (23), Gray-Level Run-Length Matrix (24), Gray-Level Size Zone Matrix (25), and Neighborhood Gray-Tone Difference Matrix (26). Features (i)-(v) have shown association with survival prediction using Adv-mpMRI scans (6). We refer to these as initial feature panel (IFP) and to the complete set as augmented feature panel (AFP).

We hypothesize that the necessary information to conduct our classification task is encapsulated by a subset of the 1612 features. Therefore, we consider the selection of the most important features as critical, to minimize the classification error and eliminate redundancy. Specifically, a forward-selection framework is used to rank and select a subset of features, based on the classification performance of a support vector machine (SVM),

using a 5-fold cross validation configuration with convergence criteria of 100 iterations and a tolerance of 10^{-4} in the classifier's performance.

2.4 Predictive Modeling

The problem of survival prediction is approached as a binary classification problem, between long and short survivors, using a formulation of two multivariate SVM classifiers (SVC), similarly to (6). One SVC model distinguishes patients that survived <12 months against others (“*short-SVC*”), and another distinguishes patients that survived >14 months against others (“*long-SVC*”). The decisions of these classifiers are then combined; a) patients classified by both classifiers as short-survivors are assigned a label of short-survivors, b) patients classified by both models as long-survivors are assigned a label of long-survivors, c) patients classified as long-survivors by the short-SVC and as short-survivors by the long-SVC are given the label of the intermediate survivor, and d) patients for which the two classifiers disagree are given a label based on the dominant distance from the two SVM hyper-planes. The generalization performance was validated using 5-fold cross-validation, to provide unbiased performance estimates. Short-and long-survivors were proportionally and randomly divided into 5 non-overlapping smaller equally sized datasets and during each fold, 4 of these subsets were considered to be the discovery/retrospective cohort and 1 as the replication/prospective cohort, which is unseen for this specific fold.

3. RESULTS

3.1 Accuracy results

The obtained cross-validated accuracies for classifying glioblastoma patients in short-, intermediate- and long-survivors, when using the a) ‘IFP Advanced’, b) ‘IFP Basic’, and c) ‘AFP Basic’ model, were equal to 60.89%, 72.77%, and 74.26%, respectively (Table 1). We evaluated the performance of the 3-class classification (described in Section 2.4) using the ‘IFP Advanced’ model, similar to our previous work (6), and obtained accuracy of 72.77% (Table 1). We next evaluated the performance of using the ‘IFP Basic’ model, which resulted in a notable decrement in performance, returning an accuracy of 60.89%. Finally, we utilized the ‘AFP Basic’ model, which resulted in a classification accuracy of 74.26%.

3.2 Feature selection

We analyzed the features selected by the nested 5-fold cross-validation, to determine if the various predictive models actually select features from the varying configurations, as well as to identify which features are selected. Indeed, it is noted that the ‘IFP Advanced’ model selected 69.57% of its features from the basic MRI protocol and 30.43% from the advanced MRI protocol. Furthermore, the ‘AFP Basic’ model revealed that 73% of its selected features were obtained from the AFP and the remainder 27% from the IFP.

3.3 Kaplan-Meier analysis

Using the ‘IFP Advanced’, the median±standard deviation OS of the short and long survivors was 9.1 ± 7.7 mts and 14.9 ± 11.3 mts, respectively. The hazard ratio for death, for short vs long, was 2.02 (95% CI:1.67–2.44). Using ‘IFP Basic’, the median±standard deviation OS of the short and long survivors was 9.2 ± 8.8 mts and 14.2 ± 11.8 mts, respectively.

Hazard ratio for death was 1.74 (95% CI:1.45–2.10). Using the ‘AFP Basic’, the median \pm standard deviation OS of the short and long survivors was 5.1 ± 3.9 mts and 16.6 ± 14.8 mts, respectively. Hazard ratio was 2.84 (95% CI:2.42–3.34) (Fig. 1).

4. DISCUSSION

Although the widespread adoption of MRI for the diagnosis and management of brain tumors such as glioblastoma has generated large datasets for imaging scientists, the most sophisticated research platforms have been established in affiliation with cancer centers utilizing Adv-mpMRI acquisition protocols, such as DTI and DSC volumes. In prior work we developed a survival prediction model using radiomic features (described here as IFP) derived from an Adv-mpMRI acquisition protocol (6). In the present work, we demonstrated that a predictive classification model using an augmented feature panel (AFP), including morphology and texture (radiomic) features, derived only from Bas-mpMRI acquisition protocols, can achieve similar results to models using the IFP derived from Adv-mpMRI acquisition protocols.

We emphasize that the strength of the presented predictive models is the potential for generalizability to patients undergoing Bas-mpMRI scanning. We replicated (6) using the ‘IFP Advanced’ model, but with different survival thresholds. We then created the ‘AFP Basic’ model and observed the best performance in stratifying patients to long-, intermediate-, and short-survivors (Table 1).

Limitations of this work include the lack of independent prospective evaluation of our method. However, this comprises a future direction; we hope that by demonstrating the feasibility of building successful classifiers from Bas-mpMRI, we may elicit collaboration with imaging scientists from other institutions to prospectively validate these findings.

We hypothesize that a model providing a stronger survival estimate would provide great benefit, as patients and clinicians make decisions on how aggressively to treat this difficult disease. Furthermore, it may be useful in stratifying / selecting patients for clinical trials, allowing for fewer patients to be needed to demonstrate effect of a novel therapeutic intervention.

5. CONCLUSION

This study has shown evidence of the feasibility of survival prediction in glioblastoma patients using solely Bas-mpMRI, which are more widely available in community settings, and integrative advanced radiomic features, indicating that such features can compensate for the lack of Adv-mpMRI. Further studies including multi-institutional data are required to prove further generalizability of our findings and evaluate application of our predictive model to MRI protocols of current clinical practice in various institutions. This method holds promise to assist clinical decision making for patients with *de novo* glioblastoma to better select patients for potentially toxic therapies and clinical trials.

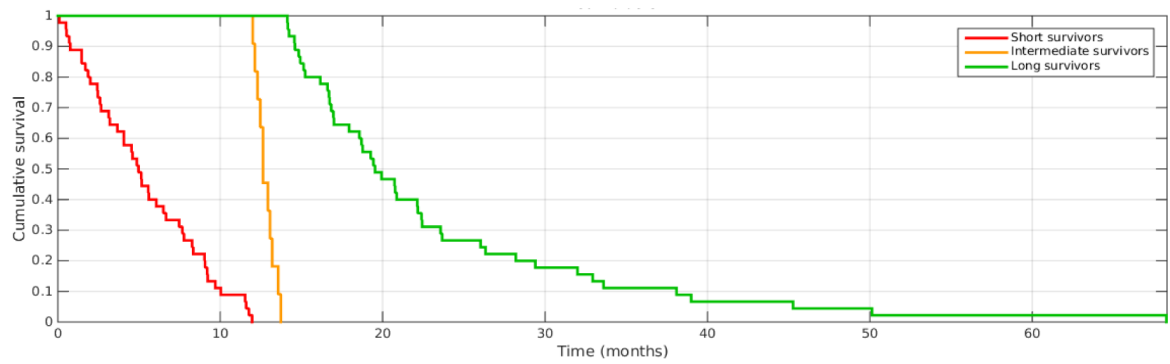
FUNDING:

This work was supported by the National Institutes of Health grants R01-NS042645 and U24-CA189523.

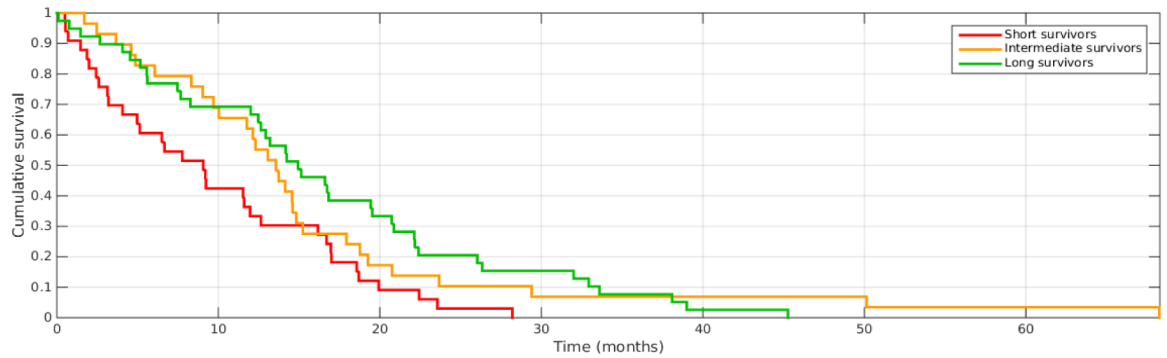
REFERENCES

1. Johnson DR, and O'Neill BP, "Glioblastoma survival in the United States before and during the temozolomide era," *Journal of Neuro-Oncology* 107(2), 359–364 (2011). [PubMed: 22045118]
2. Itakura H et al., "Magnetic resonance image features identify glioblastoma phenotypic subtypes with distinct molecular pathway activities," *Science Translational Medicine* 7(303), 303ra138–303ra138 (2015).
3. Menze BH et al., "The Multimodal Brain Tumor Image Segmentation Benchmark (BRATS)," *IEEE Transactions on Medical Imaging* 34(10), 1993–2024 (2015). [PubMed: 25494501]
4. Jaffe CC, "Imaging and Genomics: Is There a Synergy?," *Radiology* 264(2), 329–331 (2012). [PubMed: 22821693]
5. Mahajan A et al., "Radiogenomics of glioblastoma: a window into its imaging and molecular variability," *Cancer Imaging* 15(1), P14 (2015).
6. Macyszyn L et al., "Imaging patterns predict patient survival and molecular subtype in glioblastoma via machine learning techniques," *Neuro-Oncology* 18(3), 417–425 (2016). [PubMed: 26188015]
7. Aerts HL, "The potential of radiomic-based phenotyping in precision medicine: A review," *JAMA Oncology* 2(12), 1636–1642 (2016). [PubMed: 27541161]
8. Bakas S et al., "In vivo detection of EGFRvIII in glioblastoma via perfusion magnetic resonance imaging signature consistent with deep peritumoral infiltration: the ϕ -index," *Clinical Cancer Research* 23(16), 4724–4734 (2017). [PubMed: 28428190]
9. Shukla G et al., "Advanced magnetic resonance imaging in glioblastoma: a review," (2017).
10. Stupp R et al., "Effects of radiotherapy with concomitant and adjuvant temozolomide versus radiotherapy alone on survival in glioblastoma in a randomised phase III study: 5-year analysis of the EORTC-NCIC trial," *The Lancet Oncology* 10(5), 459–466 (2009). [PubMed: 19269895]
11. Gilbert MR et al., "Dose-Dense Temozolomide for Newly Diagnosed Glioblastoma: A Randomized Phase III Clinical Trial," *Journal of Clinical Oncology* 31(32), 4085–4091 (2013). [PubMed: 24101040]
12. Cox DR, "Regression Models and Life-Tables," in *Breakthroughs in Statistics: Methodology and Distribution* Kotz S, and Johnson NL, Eds., pp. 527–541, Springer New York, New York, NY (1992).
13. Bakas S et al., "Advancing The Cancer Genome Atlas glioma MRI collections with expert segmentation labels and radiomic features," *Nature Scientific Data* 4(170117), (2017).
14. Bakas S et al., "GLISTRboost: Combining Multimodal MRI Segmentation, Registration, and Biophysical Tumor Growth Modeling with Gradient Boosting Machines for Glioma Segmentation," *Brainlesion: Glioma, Multiple Sclerosis, Stroke and Traumatic Brain Injuries* 9556(144–155 (2016).
15. Hoge C, Davatzikos C, and Biros G, "An image-driven parameter estimation problem for a reaction-diffusion glioma growth model with mass effects," *Journal of Mathematical Biology* 56(6), 793–825 (2008). [PubMed: 18026731]
16. Friedman JH, "Greedy function approximation: a gradient boosting machine," *Annals of statistics* 1189–1232 (2001).
17. Bakas S et al., "Fast Semi-Automatic Segmentation of Focal Liver Lesions in Contrast-Enhanced Ultrasound, Based on a Probabilistic Model," *TCIV Computer Methods in Biomechanics and Biomedical Engineering: Imaging & Visualization* 5(5), 29–338 (2017).
18. Davatzikos C et al., "Cancer imaging phenomics toolkit: quantitative imaging analytics for precision diagnostics and predictive modeling of clinical outcome," 21 (2018).
19. Zwanenburg A et al., "Image biomarker standardisation initiative," in *ArXiv e-prints* (2016).
20. Bilello M et al., "Population-based MRI atlases of spatial distribution are specific to patient and tumor characteristics in glioblastoma," *NeuroImage Clinical* 12(34–40 (2016).

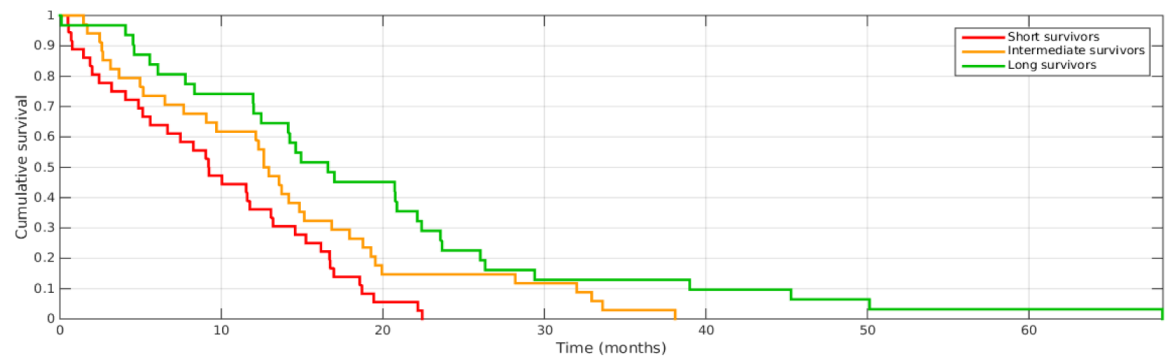
21. Hogeia C et al., "A robust framework for soft tissue simulations with application to modeling brain tumor mass effect in 3D MR images," *Physics in medicine and biology* 52(23), 6893 (2007). [PubMed: 18029982]
22. Max J, "Quantizing for minimum distortion," *IRE Transactions on Information Theory* 6(1), 7–12 (1960).
23. Haralick RM, Shanmugam K, and Dinstein I, "Textural Features for Image Classification," *IEEE Transactions on Systems, Man, and Cybernetics SMC-3*(6), 610–621 (1973).
24. Galloway MM, "Texture analysis using gray level run lengths," *Computer graphics and image processing* 4(2), 172–179 (1975).
25. Chu A, Sehgal CM, and Greenleaf JF, "Use of gray value distribution of run lengths for texture analysis," *Pattern Recognition Letters* 11(6), 415–419 (1990).
26. Amadasun M, and King R, "Textural features corresponding to textural properties," *IEEE Transactions on systems, man, and Cybernetics* 19(5), 1264–1274 (1989).



(a) KM curves using the real survival class



(b) KM curves using the 'IFP Advanced' model



(c) KM curves using the 'AFP Basic' model

Fig. 1. Kaplan Meier (KM) curves on the provided patient data for their classification on short- (<12 months), intermediate- (between 12 and 14 months), and long- survivors (>14 months), based on the real labels (a), the 'IFP Advanced' model (b), and the 'AFP Basic' model (c).

Table 1.

Accuracy for predicting survival in glioblastoma patients based on various configurations of MRI acquisition protocols, features, and for the short-SVC and long-SVC. IFP and AFP stands for Initial and Augmented Feature Panel, respectively.

Predictive Model	MRI Acquisition Protocol	Features	Accuracy	Short-SVC			Long-SVC		
				Accuracy	Sensitivity	Specificity	Accuracy	Sensitivity	Specificity
IFP Advanced	Adv-mpMRI	IFP	72.77%	66.34%	55.56%	75%	60.39%	51.11%	67.86%
IFP Basic	Bas-mpMRI	IFP	60.89%	63.37%	48.89%	75%	56.44%	35.56%	73.21%
AFP Basic	Bas-mpMRI	AFP	74.26%	62.38%	51.11%	71.43%	62.38%	48.89%	73.21%